VŠB - Technická univerzita Ostrava
Univerzitní studijní programy

Modelování anizotropních tenkovrstevných laserových struktur

Modeling of anisotropic thin-film laser structures

Author: Bc. Tibor Fördös

Supervisor: doc. Dr. Mgr. Kamil Postava

2013

VŠB - Technical University of Ostrava
University Study Programmes
Institute of Physics

Diploma Thesis Assignment

Student:	**Bc. Tibor Fördös**
Study Programme:	N3942 Nanotechnology
Study Branch:	3942T001 Nanotechnology
Title:	Modelování anizotropních tenkovrstevných laserových struktur Modeling of anisotropic thin-film laser structures

Description:

Rozvoj technologií moderních světelných emisních diod (LED) a polovodičových laserů vyžaduje rozšíření popisu šíření elektromagnetického záření na anizotropní struktury. Využití spinově polarizovaných proudů ke generaci světla a jeho průchodu přes magnetooptické vrstvy je nadějné pro rozvoj světelných zdrojů s definovaným polarizačním stavem. Základní cíle práce je možné shrnout do následujících bodů:
1. maticový popis šíření světla anizotropní a magnetooptickou tenkovrstvou strukturou
2. popis aktivní emitující vrstvy
3. modelování typických konfigurací světelných emisních diod (LED) a laserů emitujících z povrchu (VCSEL) s magnetooptickými vrstvami.

Recent technology development of modern light emitting diodes (LED) and semiconductor lasers requires generalization of electromagnetic radiation propagation description to anisotropic structures. Application of spin-polarized currents for light generation and transmission through magneto-optic films is promising for development of light sources with defined polarization state. Basic targets of the master thesis are summarized in the following items:
1. matrix description of light propagation in anisotropic and magneto-optical thin-film structures
2. description of emitting layer
3. modeling of typical configurations of light emitting diodes (LED) and vertical cavity surface emitting lasers (VCSEL) with magneto-optical films.

References:

[1] M. Holub, P. Bhattacharya, Spin-polarized light/emitting diodes and lasers, J. Phys. D: Appl. Phys. 40 (2007) R171-R203.
[2] N. C. Gerhardt and M. R. Hofmann, Spin-controlled vertical-cavity surface-emitting lasers, Advances in Optical Technologies, Vol. 2012, 268949, Hindawi Publishing Corporation, 2012.
[3] H. Benisty, R. Stanley, and M. Mayer, Method of source terms for dipole emission modification in modes of arbitrary planar structures, J. Opt. Soc. Am. A, Vol. 15, pp. 1192-1201, May 1998.
[4] R. Baets, P. Bienstman, and R. Bockstaele, Basics of dipole emission from a planar cavity, Lecture Notes in Physics, Springer Berlin 1999, pp. 38-79.
[5] Š. Višňovský, Optics of magnetic multilayers and nanostructures,
Taylor & Francis, CRC Press 2006.
[6] P. Yeh, Optical waves in layered media, John Wiley & Sons, New York,1988.

Extent and terms of a thesis are specified in directions for its elaboration that are opened to the public on the web sites of the faculty.

Supervisor: **doc. Dr. Mgr. Kamil Postava**

Date of issue: 16. 11. 2012

Date of submission: 15. 05. 2013

prof. Dr. RNDr. Jiří Luňáček
Head of Department

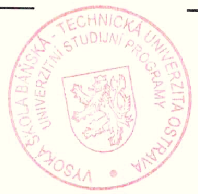

prof. Ing. Petr Noskievič, CSc.
Vice-rector for Study Affairs

Prohlášení

- Byl(a) jsem seznámen(a) s tím, že na moji diplomovou práci se plně vztahuje zákon č.121/2000 Sb. - autorský zákon, zejména § 35 - využití díla v rámci občanských a náboženských obřadů, v rámci školních představení a využití díla školního a § 60 - školní dílo.

- Beru na vědomí, že Vysoká škola báňská - Technická univerzita Ostrava (dále jen VŠB-TUO) má právo nevýdělečně, ke své vnitřní potřebě, diplomovou práci užít (§ 35 odst. 3).

- Souhlasím s tím, že jeden výtisk diplomové práce bude uložen v Ústřední knihovně VŠB-TUO k prezenčnímu nahlédnutí a jeden výtisk bude uložen u vedoucího diplomové práce. Souhlasím s tím, že údaje o diplomové práci, obsažené v Záznamu o závěrečné práci, umístěném v příloze mé diplomové práce, budou zveřejněny v informačním systému VŠB-TUO.

- Bylo sjednáno, že s VŠB-TUO, v případě zájmu z její strany, uzavřu licenční smlouvu s oprávněním užít dílo v rozsahu § 12 odst. 4 autorského zákona.

- Bylo sjednáno, že užít své dílo - diplomovou práci nebo poskytnout licenci k jejímu využití mohu jen se souhlasem VŠB-TUO, která je oprávněna v takovém případě ode mne požadovat přiměřený příspěvek na úhradu nákladů, které byly VŠB-TUO na vytvoření díla vynaloženy (až do jejich skutečné výše).

- Místopřísežně prohlašuji, že celou diplomovou práci včetně příloh, jsem vypracoval(a) samostatně a uvedl(a) jsem všechny použité podklady a literaturu.

V Ostravě dne 15.5.2013 _____

Declaration

I declare I elaborated this thesis by myself. All literary sources and publications I have used had been cited.

Ostrava, May 15, 2013 _____

Abstrakt

Spinově polarizované zdroje záření jako například spinově polarizované světelné emisní diody (spin-LED) a spinově polarizované lasery (spin-lasery) jsou perspektivní zařízení v nichž zářivé rekombinace spinově polarizovaných nosičů náboje vedou k emisi fotonů s kruhovou polarizací. Hlavním cílem této práce je modelování emitovaného pole a polarizačních vlastností spin-LED struktur a spinových laserů s vertikálním uspořádáním (spin-VCSEL). Je odvozen nový přístup založený na 4×4 maticovém formalismu, který popisuje interakci světla s rezonanční multivrstevnou strukturou. Kvantové přechody, které vedou k emisi fotonů, jsou popsány Jonesovými zdrojovými vektory.

Abstract

Spin-polarized light sources such as the spin-polarized light-emitting diodes (spin-LEDs) and spin-polarized lasers (spin-lasers) are perspective devices in which the radiative recombinations of spin-polarized carriers result in emission of circularly polarized photons. Main goal of this thesis is modeling outside emited field and polarization properties of spin-LED and spin-controled vertical-cavity surface-emiting laser (spin-VCSEL) structures. New approach based 4×4 matrix formalism is derived for modeling of light interaction in resonant multilayer structure. Quantum transitions, which result in photon emission, are described using Jones source vectors.

Contents

Nomenclature

$A^{(n)}$	wave amplitude in the n-th layer
$\mathbf{B}$	magnetic flux density
$\mathbf{D}$	electric displacement
$\mathbf{D}^{(n)}$	dynamic matrix of the n-th layer
$\hat{\mathbf{D}}$	dipole moment operator
$\mathbf{E}$	electric field intensity
$\mathbf{H}$	magnetic field intensity
$\mathbf{J}$	total angular momentum of the electron
$\mathbf{J}^d_{\uparrow\downarrow}$	Jones vector of the source
$\boldsymbol{M}$	magnetization vector
$\mathbf{M}$	total matrix
N_x, N_y, N_z	effective refractive index components
$\mathbf{P}^{(n)}$	propagation matrix of the n-th layer
$d^{(n)}$	thickness of the n-th layer
$\mathbf{e}^{(n)}$, $\mathbf{h}^{(n)}$	normalized eigen-polarization in the n-th layer
$\mathbf{j}$	current density
k	wave number
m_j	magnetic quantum number
$n_\pm$	density of electrons in $\pm 1/2$
t	time
$\widehat{x}$, $\widehat{y}$, $\widehat{z}$	unit vectors
γ	weight coefficient of spontaneous emission
δ	weight coefficient of stimulated emission
$\hat{\varepsilon}^{(n)}$	permitivitty tensor of the n-th layer
ω	angular frequency of monochromatic wave
ψ_{km}	Bloch wave function
ξ_{hh}, ξ_{lh}	transition probability including heavy holes and light holes

Chapter 1

Introduction

Spin-polarized light sources such as the spin-polarized light-emitting diodes (spin-LEDs) and spin-polarized lasers (spin-lasers) are perspective devices in which the radiative recombinations of spin-polarized carriers result in emission of circularly polarized photons. The connection between spin polarization of the charge carriers and optical polarization of the emitted photons can be applied in many practical areas. In experimental spintronics, spin-LEDs are already used for detection and characterization of spin-polarized carriers in novel spintronic structures [1, 2, 3, 4]. Spin-lasers promise lower threshold [5, 6], faster modulation dynamics [7], improved polarization stability and polarization determination [8, 9]. Moreover, the ability to control modulated light polarization together with improved properties opens new horizons in laser technology, cryptography and modern optical components.

For the above applications, a precise modeling of light emission from multilayer structure with active layer is needed. It could be based on two steps: (i) Representation of active layer by using dipole sources and (ii) Modeling of light emission in resonant multilayer structure by using appropriate matrix approach fulfilling Maxwell equations in each layer and boundary conditions for electromagnetic field. It is well established that spontaneous emission in a semiconductor can be represented as an electric dipole emission in the so-called weak-coupling regime. When atoms in the active area spontaneously emit electromagnetic radiation, each atom acts like a small randomly oscilating electric dipole with the frequency of the transition. If the emission is stimulated, each atom acts like a miniature passive resonant electric dipole, which is set oscilating by the incident wave and hence oscilation is not random but is coherent with the incident wave [10]. In the case of the resonant-cavity LED (RCLED), the active layer is embeded in a multilayer nanostructure [11]. Optical interaction of the dipole field and the isotropic multilayer

structure was efectively described by Benisty [12] by using transfer matrix formalism, while the vectorial problem of the dipole emission was decomposed in three scalar problems: *s*- and *p*-field generated by a dipole paralel to the interface and *p*-field generated by a dipole, which is perpendicular to the interfaces. This approach enables to calculate both field amplitudes radiated from the structure as well as field in any point of the structure.

However, in the spin-LEDs and spin-lasers, spin polarization of the carriers is directly related to the optical polarization of the emited photons through the quantum selection rules. Moreover, the magnetic field used for electric current polarization causes anisotropic magneto-optical effects and *s*-*p* conversion. Main goal of this thesis is modeling outside emited field and polarization properties of spin-LED and spin-controled vertical-cavity surface-emiting laser (spin-VCSEL) structures. In Chapter 2, we first introduce the 4x4 Yeh's matrix formalism for anisotropic multilayer structure including active source layer, which is described by general source amplitude vector. Considering the anisotropy is very important because of presense of the external magnetic field in spin-optoelectronics devices. In Chapter 3, we discuss particular form of the source amplitude distribution of the active layer, which are directly related to the quantum optical selection rules. We introduce method of two crossed linear sources emitting circularly polarized light with parameters, which could be obtained by fitting experimental data or using theory. Chapter 4 shows application of general approach to typical spin-VCSEL structures.

Chapter 2

Electromagnetic response of multilayer structure

In this chapter, the 4×4 Yeh's matrix formalism is described [13]. This formalism provides effective mathematical method for description of electromagnetic response of anisotropic multilayered system. The main part of this chapter deals with the new approach for modeling of anisotropic multilayer systems, which include active source layer defined by general Jones vectors representing quantum transitions.

2.1 Wave equation for the anisotropic media

The Maxwell equations are partial differential equations, which describe classical properties of the electromagnetic field and can be written in the following diferential form

$$\operatorname{div} \mathbf{D} = \rho \tag{2.1}$$

$$\operatorname{div} \mathbf{B} = 0 \tag{2.2}$$

$$\operatorname{rot} \mathbf{E} = -\frac{\partial \mathbf{B}}{\partial t} \tag{2.3}$$

$$\operatorname{rot} \mathbf{H} = \mathbf{j} + \frac{\partial \mathbf{D}}{\partial t}\,, \tag{2.4}$$

where $\mathbf{E}$, $\mathbf{H}$, $\mathbf{D}$, $\mathbf{B}$, ρ, and $\mathbf{j}$ denote the electric field intensity, the magnetic field intensity, the electric displacement, the magnetic flux density, the volume density of the free charges, and the current density, respectively. For a monochromatic plane wave solution with the

propagation vector $\mathbf{k}$, the field vectors can be expressed as

$$\mathbf{E}(\mathbf{r},t) = \Re\{\mathbf{E_0}\exp[i(\omega t - \mathbf{kr})]\} \quad (2.5)$$
$$\mathbf{H}(\mathbf{r},t) = \Re\{\mathbf{H_0}\exp[i(\omega t - \mathbf{kr})]\}, \quad (2.6)$$

where ω is the angular frequency. The time course of the direction of $\mathbf{E}(r,t)$ determines polarization state of the light, which is commonly described in Cartesian coordinates using Jones vector

$$\mathbf{J} = \begin{bmatrix} E_{x0} \\ E_{y0} \end{bmatrix}, \quad (2.7)$$

where E_{x0} and E_{y0} are the x and y components of the complex amplitude $\mathbf{E_0}$ in the case of a wave propagating in the z-direction [14]. We define s- and p- polarizations (see Fig 2.1) and the reflections coefficient

$$r_{ij} = \frac{E_{0j}}{E_{0i}}, \quad (2.8)$$

where the indices denote i (incident $s-$ or $p-$) and j(reflected $s-$ or $p-$) polarized wave.

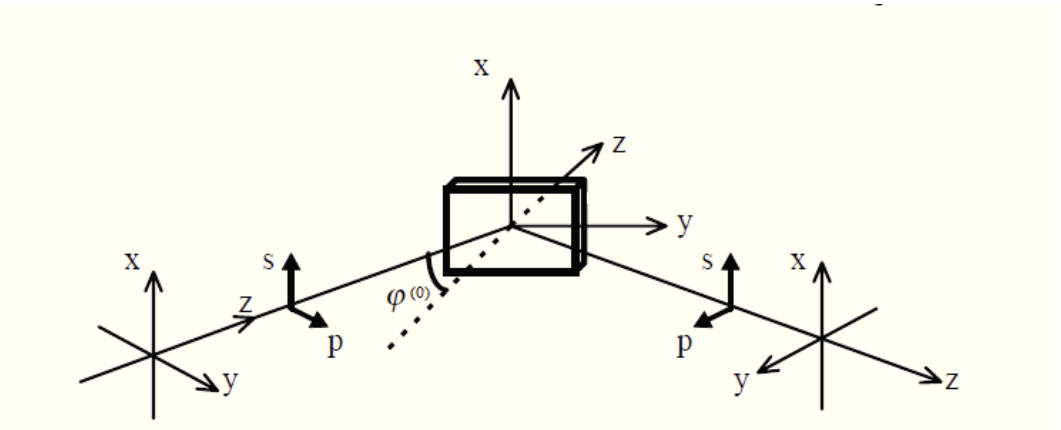

Figure 2.1: S-polarization lies along x-axis - perpendicular to the plane of incidence. P-polarization lies in the plane of incidence.

By substituting (2.5) and (2.6) into last two Maxwell equations (2.3) and (2.4), we obtain the condition for the complex amplitudes $\mathbf{E_0}$ and $\mathbf{H_0}$

$$\mathbf{k} \times \mathbf{E_0} - \omega\mu_0\hat{\mu}\mathbf{H_0} = 0 \quad (2.9)$$
$$\mathbf{k} \times \mathbf{H_0} + \omega\varepsilon_0\hat{\varepsilon}\mathbf{E_0} = 0,$$

where ε_0 and μ_0 denotes the vacuum permittivity and permeability Note, that for optical frequencies the permeability tensor $\hat{\mu} \approx 1$. After eliminating $\mathbf{H}$, we obtain the wave equation in the form

$$k_0\hat{\varepsilon}\mathbf{E_0} - \mathbf{k^2E_0} + \mathbf{k}(\mathbf{kE_0}) = 0, \tag{2.10}$$

where the permittivity tensors $\hat{\varepsilon}$ decribe anisotropy of the enviroment and can be generally written in the form

$$\hat{\varepsilon} = \begin{pmatrix} \varepsilon_{xx} & \varepsilon_{xy} & \varepsilon_{xz} \\ \varepsilon_{yx} & \varepsilon_{yy} & \varepsilon_{yz} \\ \varepsilon_{zx} & \varepsilon_{zy} & \varepsilon_{zz} \end{pmatrix}. \tag{2.11}$$

In the case of cubic crystal, we can distinguish three basic configuration of linear magneto-optical tensor in relation with the direction of the magnetization $\mathbf{M}$:

1. Polar geometry with the magnetization in z-direction

$$\hat{\varepsilon}_{polar} = \begin{pmatrix} \varepsilon_{xx} & -i\varepsilon_{xy}(M_z) & 0 \\ i\varepsilon_{xy}(M_z) & \varepsilon_{xx} & 0 \\ 0 & 0 & \varepsilon_{xx} \end{pmatrix} \tag{2.12}$$

2. Longitudinal geometry with the magnetization in y-direction

$$\hat{\varepsilon}_{longitudinal} = \begin{pmatrix} \varepsilon_{xx} & 0 & i\varepsilon_{xz}(M_y) \\ 0 & \varepsilon_{xx} & 0 \\ -i\varepsilon_{xz}(M_y) & 0 & \varepsilon_{xx} \end{pmatrix} \tag{2.13}$$

3. Transverse geometry with the magnetization in x-direction

$$\hat{\varepsilon}_{transverse} = \begin{pmatrix} \varepsilon_{xx} & 0 & 0 \\ 0 & \varepsilon_{xx} & -i\varepsilon_{yz}(M_x) \\ 0 & i\varepsilon_{yz}(M_x) & \varepsilon_{xx} \end{pmatrix}. \tag{2.14}$$

Note, that the Jones vector defined by (2.7) only spans the space of fully polarized light. However, it's common to define the Stokes vector

$$\mathbf{S} = \begin{pmatrix} S_0 \\ S_1 \\ S_2 \\ S_3 \end{pmatrix} = \begin{pmatrix} I_0 \\ I_x - I_y \\ I_{45} - I_{-45} \\ I_{RP} - I_{LP} \end{pmatrix}, \tag{2.15}$$

which shows the light intensities of different polarization states and could describe unpolarized, partially polarized, and fully polarized light. The Stokes parameters are defined by following:

- $S_0 = I_0$ ... total intensity,
- $S_1 = I_0 = I_x - I_y$ ... intensity diference between vertically and horizontally polarized light,
- $S_2 = I_{45} - I_{-45}$ ... intensity diference between light linearly polarized along the plane with angle $\pm 45°$ about the x-plane,
- $S_3 = I_{RP} - I_{LP}$ ... intensity diference between right and left circularly polarized light.

Moreover, the portion of an electromagnetic wave, which is polarized, can be described by the degree of polarization defined by

$$\mathcal{P} = \frac{\sqrt{S_1^2 + S_2^2 + S_3^2}}{S_0}, \tag{2.16}$$

which for totally polarized, unpolarized, and partially polarized light is equal to $\mathcal{P} = 1$, $\mathcal{P} = 0$, and $0 < \mathcal{P} < 1$, respectively.

2.2 Matrix formalism

Let us consider anisotropic multilayer structure consisting of N-anisotropic layers characterized by permittivity tensors $\hat{\varepsilon}^{(n)}$ and the thicknesses $d^{(n)}$, with $n = 1, ..., N$. The interface planes are normal to a common axis parallel to the z axis of the Cartesian coordinate system. The wave equation for each layer can be written in the following form [15, 13]

$$k_0^2 \hat{\varepsilon}^{(n)} \mathbf{E_0}^{(n)} - \mathbf{k}^{2(n)} \mathbf{E_0}^{(n)} + \mathbf{k}^{(n)} [\mathbf{k}^{(n)} \mathbf{E_0}^{(n)}] = 0, \tag{2.17}$$

where $\mathbf{E_0}^{(n)}$ is the amplitude of the electric field in each layer $\mathbf{E}^{(\mathrm{n})} = \mathbf{E}_0^{(\mathrm{n})} \mathrm{e}^{\mathrm{i}(\omega \mathrm{t} - \mathbf{k}^{(\mathrm{n})} \mathbf{r})}$. Because of the Snell's law, the wave propagates in each medium with the same tangential component of the wave vector $\mathbf{k}^{(n)} = k_0(N_x \widehat{\mathbf{x}} + N_y \widehat{\mathbf{y}} + N_z^{(n)} \widehat{\mathbf{z}})$. Let us choose coordinate system, for which $N_x = 0$ and $N_y = n^{(n)} \sin \theta^{(n)} = \text{const.}$ and rewrite the wave equation (2.17) in the matrix form

$$\underbrace{\begin{pmatrix} \varepsilon_{xx}^{(n)} - N_y^2 - N_z^{(n)2} & \varepsilon_{xy}^{(n)} & \varepsilon_{xz}^{(n)} \\ \varepsilon_{yx}^{(n)} & \varepsilon_{yy}^{(n)} - N_z^{(n)2} & \varepsilon_{yz}^{(n)} + N_y N_z^{(n)} \\ \varepsilon_{zx}^{(n)} & \varepsilon_{zy}^{(n)} + N_y N_z^{(n)} & \varepsilon_{zz}^{(n)} - N_y^2 \end{pmatrix}}_{\spadesuit} \begin{bmatrix} E_{0x}^{(n)} \\ E_{0y}^{(n)} \\ E_{0z}^{(n)} \end{bmatrix} = 0, \tag{2.18}$$

where the condition for existence of nontrivial solution is ensured by fourth-order algebraic equation

$$\det(\spadesuit) = 0. \tag{2.19}$$

Four solutions $N_{zj}^{(n)}$, where $(j = 1, 3)$ and $(j = 2, 4)$, correspond to the forward and backward propagating modes called eigen-modes. The eigenmode polarizations $\mathbf{E}_{0j}^{(n)}$ are specific for each media and do not change during the propagation and take the form

$$\mathbf{E}_{0j}^{(n)} = A_j^{(n)} \mathbf{e}_{0j}^{(n)}, \tag{2.20}$$

where $A_j^{(n)}$ is the amplitude of particular wave and $\mathbf{e}_{0j}^{(n)}$ is the normalized eigen-polarization satisfying

$$\left[\mathbf{e}_{0j}^{(n)}\right]^{+} \mathbf{e}_{0j}^{(n)}, \tag{2.21}$$

where $\left[\mathbf{e}_{0j}^{(n)}\right]^{+}$ denotes Hermitian adjoint. Inside n-th layer at the interface $n/n+1$, we express the field vector $\mathbf{E}^{(n)}$ as a linear combination of these eigen-polarizations

$${}^{(n/n+1)}\mathbf{E}_0^{(n)} = \sum_{j=1}^{4} A_j^{(n)} \mathbf{e}_{0j}^{(n)}. \tag{2.22}$$

The propagation in the n-th layer change the field vector according to a factor $\exp[ik_0 N_{zj}^{(n)} d^{(n)}]$

$${}^{(n-1/n)}\mathbf{E}_0^{(n)} = \sum_{j=1}^{4} A_j^{(n)} \mathbf{e}_{0j}^{(n)} \exp[ik_0 N_{zj}^{(n)} d^{(n)}]. \tag{2.23}$$

The boundary conditions require continuity of tangential components of the field vectors $\mathbf{E}$ and $\mathbf{H}$ at the interface

$$\begin{aligned} {}^{(n-1/n)}\mathbf{E}_{0x}^{(n)} &= {}^{(n-1/n)}\ \mathbf{E}_{0x}^{(n-1)},\ {}^{(n-1/n)}\mathbf{E}_{0y}^{(n)} = {}^{(n-1/n)}\ \mathbf{E}_{0y}^{(n-1)}, \\ {}^{(n-1/n)}\mathbf{H}_{0x}^{(n)} &= {}^{(n-1/n)}\ \mathbf{H}_{0x}^{(n-1)},\ {}^{(n-1/n)}\mathbf{H}_{0y}^{(n)} = {}^{(n-1/n)}\ \mathbf{H}_{0y}^{(n-1)}, \end{aligned}$$

and in the matrix form take the form

$$\mathbf{D}^{(n-1)} \mathbf{A}^{(n-1)} = \mathbf{D}^{(n)} \mathbf{P}^{(n)} \mathbf{A}^{(n)},$$

where $\mathbf{D}^{(n)}$ (Dynamical matrix) and $\mathbf{P}^{(n)}$ (Propagation matrix) have the following form

$$\mathbf{D}^{(n)} = \begin{pmatrix} \mathbf{e}_{x1}^{(n)} & \mathbf{e}_{x2}^{(n)} & \mathbf{e}_{x3}^{(n)} & \mathbf{e}_{x4}^{(n)} \\ \mathbf{h}_{y1}^{(n)} & \mathbf{h}_{y2}^{(n)} & \mathbf{h}_{y3}^{(n)} & \mathbf{h}_{y4}^{(n)} \\ \mathbf{e}_{y1}^{(n)} & \mathbf{e}_{y2}^{(n)} & \mathbf{e}_{y3}^{(n)} & \mathbf{e}_{y4}^{(n)} \\ \mathbf{h}_{x1}^{(n)} & \mathbf{h}_{x2}^{(n)} & \mathbf{h}_{x3}^{(n)} & \mathbf{h}_{x4}^{(n)} \end{pmatrix}, \quad \mathbf{A}^{(n)} = \begin{bmatrix} A_1^{(n)} \\ A_2^{(n)} \\ A_3^{(n)} \\ A_4^{(n)} \end{bmatrix} \tag{2.24}$$

$$\mathbf{P}^{(n)} = \begin{pmatrix} ik_0 N_{z1}^{(n)} d^{(n)} & 0 & 0 & 0 \\ 0 & ik_0 N_{z2}^{(n)} d^{(n)} & 0 & 0 \\ 0 & 0 & ik_0 N_{z3}^{(n)} d^{(n)} & 0 \\ 0 & 0 & 0 & ik_0 N_{z4}^{(n)} d^{(n)} \end{pmatrix}. \tag{2.25}$$

Using $\mathbf{P}^{(n)}$ and $\mathbf{D}^{(n)}$, the amplitudes in the halfspaces (0) and $(N+1)$ can be related in the following form

$$\mathbf{A}^{(0)} = \underbrace{\left[\mathbf{D}^{(0)}\right]^{-1} \mathbf{D}^{(1)} \mathbf{P}^{(1)} \ldots \left[\mathbf{D}^{(N)}\right]^{-1} \mathbf{D}^{(N+1)} \mathbf{P}^{(N+1)}}_{\mathbf{M}} \mathbf{A}^{(N+1)}, \tag{2.26}$$

where $\mathbf{M}$ is the total matrix of the system.

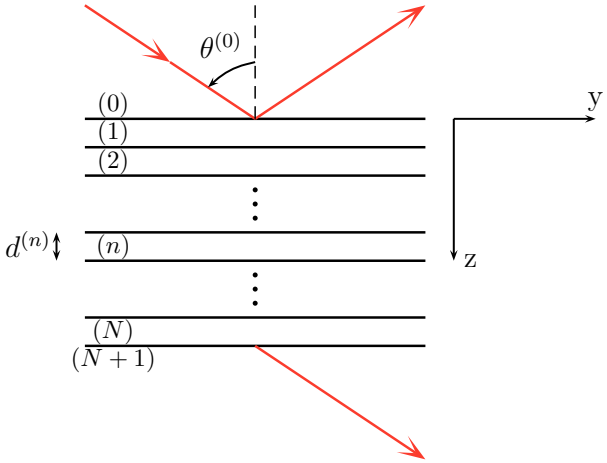

Figure 2.2: Multilayer structure embeded in isotropic halfspaces (0) and $(N+1)$. Each layer is characterized by the permitivitty tensor $\hat{\varepsilon}^{(n)}$ and the thickness $d^{(n)}$.

Note, that in the case of isotropic layered media, the electromagnetic field can be divided into two uncoupled modes: s-modes and p-modes with electric field vector perpendicular and parallel to the plane of incidence, respectively. Since they are uncoupled,

characteristic equation for $N_{z,j}^{(n)}$ biquadratic with solution

$$N_{z,1,3}^{(n)} = N_{z,2,4}^{(n)} = n^{(n)}\cos\theta^{(n)}, \tag{2.27}$$

and the dynamic matrix takes the block diagonal form

$$\mathbf{D} = \begin{pmatrix} 1 & 1 & 0 & 0 \\ n^{(n)}\cos\theta^{(n)} & -n^{(n)}\cos\theta^{(n)} & 0 & 0 \\ 0 & 0 & \cos\theta^{(n)} & \cos\theta^{(n)} \\ 0 & 0 & -n^{(n)} & n^{(n)} \end{pmatrix}. \tag{2.28}$$

2.3 New approach for spin-LED and spin-VCSEL structures

The 4x4 Yeh's matrix formalism provides effective approach for investigation of the propagation of electromagnetic radiation in anisotropic layered media, where each layer is characterized by the complex relative permittivity tensor $\hat{\varepsilon}^{(n)}$. In the case of anisotropic layered media, the field in a individual layer can be expressed as a linear superposition of monochromatic plane waves with four proper polarization, which are obtained by nontrivial solution of wave equation in each anisotropic layer. The boundary conditions, which require continuity of tangential components of the field vectors, are expressed by using a 4x4 dynamical matrix $\mathbf{D}^{(n)}$ as a relation between four field amplitudes and the corresponding four field amplitudes in the adjacent layer. Propagation of these partial waves in each each layer is described by diagonal matrix $\mathbf{P}^{(n)}$, which consists of the phase excursions [15, 13].

Let us consider the multilayer system including the isotropic layer (n) with the emitting active region (see Fig.2.4). Outside field amplitudes in the halfspaces (0) and $(N+1)$ are related to the field amplitudes on both sides of the active region by relations

$$\begin{pmatrix} A_1^{(n)\prime} \\ A_2^{(n)\prime} \\ A_3^{(n)\prime} \\ A_4^{(n)\prime} \end{pmatrix} = \begin{pmatrix} \widetilde{M}_{11}^{(u)} & \widetilde{M}_{12}^{(u)} & \widetilde{M}_{13}^{(u)} & \widetilde{M}_{14}^{(u)} \\ \widetilde{M}_{21}^{(u)} & \widetilde{M}_{22}^{(u)} & \widetilde{M}_{23}^{(u)} & \widetilde{M}_{24}^{(u)} \\ \widetilde{M}_{31}^{(u)} & \widetilde{M}_{32}^{(u)} & \widetilde{M}_{33}^{(u)} & \widetilde{M}_{34}^{(u)} \\ \widetilde{M}_{41}^{(u)} & \widetilde{M}_{42}^{(u)} & \widetilde{M}_{43}^{(u)} & \widetilde{M}_{44}^{(u)} \end{pmatrix} \begin{pmatrix} 0 \\ A_2^{(0)} \\ 0 \\ A_4^{(0)}, \end{pmatrix} \tag{2.29}$$

$$\begin{pmatrix} A_1^{(n)''} \\ A_2^{(n)''} \\ A_3^{(n)''} \\ A_4^{(n)''} \end{pmatrix} = \begin{pmatrix} M_{11}^{(d)} & M_{12}^{(d)} & M_{13}^{(d)} & M_{14}^{(d)} \\ M_{21}^{(d)} & M_{22}^{(d)} & M_{23}^{(d)} & M_{24}^{(d)} \\ M_{31}^{(d)} & M_{32}^{(d)} & M_{33}^{(d)} & M_{34}^{(d)} \\ M_{41}^{(d)} & M_{42}^{(d)} & M_{43}^{(d)} & M_{44}^{(d)} \end{pmatrix} \begin{pmatrix} A_1^{(N+1)} \\ 0 \\ A_3^{(N+1)} \\ 0 \end{pmatrix}, \tag{2.30}$$

where total matrixes are calculated in the following way

$$\widetilde{\mathbf{M}}^{(u)} = \left[\mathbf{P}^{(n)'}\right]^{-1} \left[\mathbf{D}^{(n)}\right]^{-1} \mathbf{D}^{(n-1)} \left[\mathbf{P}^{(n-1)}\right]^{-1} \dots \left[\mathbf{P}^{(1)}\right]^{-1} \left[\mathbf{D}^{(1)}\right]^{-1} \mathbf{D}^{(0)}$$

and

$$\mathbf{M}^{(d)} = \mathbf{P}^{(n)''} \left[\mathbf{D}^{(n)}\right]^{-1} \mathbf{D}^{(n+1)} \mathbf{P}^{(n+1)} \dots \mathbf{P}^{(\mathrm{N})} \left[\mathbf{D}^{(\mathrm{N})}\right]^{(-1)} \mathbf{D}^{(\mathrm{N}+1)}.$$

The matrices $\mathbf{P}^{(n)'}$ and $\mathbf{P}^{(n)''}$ are the propagation matrices of the (n)-th layer region above and below of the active plane. Let us write the complex amplitudes above and below active region in the form of the Jones vectors

$$\mathbf{J}'_{\downarrow} = \begin{pmatrix} A_1^{(n)'} \\ A_3^{(n)'} \end{pmatrix}, \quad \mathbf{J}''_{\downarrow} = \begin{pmatrix} A_1^{(n)''} \\ A_3^{(n)''} \end{pmatrix}, \quad \mathbf{J}'_{\uparrow} = \begin{pmatrix} A_2^{(n)'} \\ A_4^{(n)'} \end{pmatrix},$$

and

$$\mathbf{J}''_{\uparrow} = \begin{pmatrix} A_2^{(n)''} \\ A_4^{(n)''} \end{pmatrix}.$$

Note that the amplitudes $A_1^{(n)}$, $A_3^{(n)}$, and $A_2^{(n)}$, $A_4^{(n)}$ correspond to orthogonal eigenpolarizations.

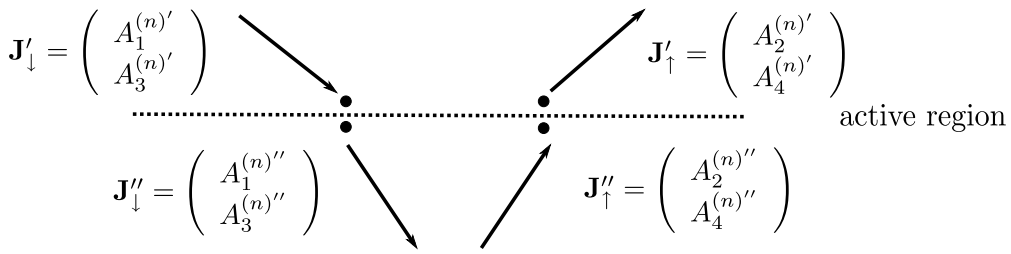

Figure 2.3: Jones vectors

Field amplitudes traveling through the source plane are amplified by interactions with the active region. First, we describe amplification of the waves propagating downwards using the Jones vector of the source $\mathbf{J}^d_{\downarrow} = [A_1^d\, A_3^d]^T$, which polarization is related to

particular quantum transition. In the case of stimulated emission, emited waves are coherent and have equivalent polarisation as the waves (or part of waves), which stimulate the emission. If the incident wave polarization $\mathbf{J}'_{\downarrow}$ is diferent from the polarization $\mathbf{J}^d_{\downarrow}$, then only a part of the wave $\mathbf{J}'_{\downarrow}$ is amplified by the stimulated emission. Therefore we express the incident Jones vector $\mathbf{J}'_{\downarrow}$ as a weighted superposition of two orthogonal Jones vectors

$$\mathbf{J}'_{\downarrow} = \alpha \mathbf{J}^d_{\downarrow} + \beta \mathbf{J}_{\downarrow}, \tag{2.31}$$

where $\mathbf{J}^d_{\downarrow} = [A^d_1\, A^d_3]^T$ is the Jones vector of the source and $\beta\mathbf{J}_{\downarrow}$ is it's orthogonal counterpart. From orthogonality reason the Hermitian product is in the form

$$\left(\mathbf{J}^d_{\downarrow}, \mathbf{J}_{\downarrow}\right) = \mathbf{J}^d_{\downarrow}\mathbf{J}^+_{\downarrow} = A^d_1 A^*_1 + A^d_3 A^*_3 = 0, \tag{2.32}$$

it follows

$$\alpha = \frac{\left(\mathbf{J}'_{\downarrow},\, \mathbf{J}^d_{\downarrow}\right)}{\left(\mathbf{J}^d_{\downarrow},\, \mathbf{J}^d_{\downarrow}\right)}\,. \tag{2.33}$$

Amplitudes traveling through the source plane are amplified in the following way

$$\mathbf{J}''_{\downarrow} = \mathbf{J}'_{\downarrow} + \alpha\delta\sqrt{\left(\mathbf{J}^{\mathbf{d}}_{\downarrow},\, \mathbf{J}^{\mathbf{d}}_{\downarrow}\right)}\mathbf{J}^d_{\downarrow} + \gamma\mathbf{J}^d_{\downarrow}, \tag{2.34}$$

where the second and third term correspond with stimulated and spontaneous emission, respectively. γ and δ represent the weight coefficients of spontaneous and stimulated emission, respectively. Thus, field amplitudes on each side of the active region are bounded by the relation

$$\mathbf{J}''_{\downarrow} = \mathbf{T}^{\downarrow}\mathbf{J}'_{\downarrow} = \begin{pmatrix} 1+\delta\frac{A^d_1 A^{d*}_1}{\sqrt{\left(\mathbf{J}^d_{\downarrow},\mathbf{J}^d_{\downarrow}\right)}} & \delta\frac{A^d_1 A^{d*}_3}{\sqrt{\left(\mathbf{J}^d_{\downarrow},\mathbf{J}^d_{\downarrow}\right)}} \\ \delta\frac{A^d_3 A^{d*}_1}{\sqrt{\left(\mathbf{J}^d_{\downarrow},\mathbf{J}^d_{\downarrow}\right)}} & 1+\delta\frac{A^d_3 A^{d*}_3}{\sqrt{\left(\mathbf{J}^d_{\downarrow},\mathbf{J}^d_{\downarrow}\right)}} \end{pmatrix}\mathbf{J}'_{\downarrow} + \gamma\mathbf{J}^d_{\downarrow} \tag{2.35}$$

and anagolously by using the source vector $\mathbf{J}^d_{\uparrow} = [A^d_2\, A^d_4]^T$ for upward propagating amplitudes

$$\mathbf{J}'_{\uparrow} = \mathbf{T}^{\uparrow}\mathbf{J}''_{\uparrow} = \begin{pmatrix} 1+\delta\frac{A^d_2 A^{d*}_2}{\sqrt{\left(\mathbf{J}^d_{\uparrow},\mathbf{J}^d_{\uparrow}\right)}} & \delta\frac{A^d_2 A^{d*}_4}{\sqrt{\left(\mathbf{J}^d_{\uparrow},\mathbf{J}^d_{\uparrow}\right)}} \\ \delta\frac{A^d_4 A^{d*}_2}{\sqrt{\left(\mathbf{J}^d_{\uparrow},\mathbf{J}^d_{\uparrow}\right)}} & 1+\delta\frac{A^d_4 A^{d*}_4}{\sqrt{\left(\mathbf{J}^d_{\uparrow},\mathbf{J}^d_{\uparrow}\right)}} \end{pmatrix}\mathbf{J}''_{\uparrow} + \gamma\mathbf{J}^d_{\uparrow}. \tag{2.36}$$

From Eq. (2.29), (2.30), (2.35), and (2.36), we obtain the system of four algebraic equations for four outside field amplitudes in the folowing form

$$\begin{pmatrix} T^{\downarrow}_{11}\widetilde{M}^{(u)}_{12} + T^{\downarrow}_{12}\widetilde{M}^{(u)}_{32} & T^{\downarrow}_{11}\widetilde{M}^{(u)}_{14} + T^{\downarrow}_{12}\widetilde{M}^{(u)}_{34} & -M^{(d)}_{11} & -M^{(d)}_{13} \\ -\widetilde{M}^{(u)}_{22} & -\widetilde{M}^{(u)}_{24} & T^{\uparrow}_{11}M^{(d)}_{21} + T^{\uparrow}_{12}M^{(d)}_{41} & T^{\uparrow}_{11}M^{(d)}_{23} + T^{\uparrow}_{12}M^{(d)}_{43} \\ T^{\downarrow}_{21}\widetilde{M}^{(u)}_{12} + T^{\downarrow}_{22}\widetilde{M}^{(u)}_{32} & T^{\downarrow}_{21}\widetilde{M}^{(u)}_{14} + T^{\downarrow}_{22}\widetilde{M}^{(u)}_{34} & -M^{(d)}_{31} & -M^{(d)}_{33} \\ -\widetilde{M}^{(u)}_{42} & -\widetilde{M}^{(u)}_{44} & T^{\uparrow}_{21}M^{(d)}_{21} + T^{\uparrow}_{22}M^{(d)}_{41} & T^{\uparrow}_{21}M^{(d)}_{23} + T^{\uparrow}_{22}M^{(d)}_{43} \end{pmatrix}\begin{pmatrix} A^{(0)}_2 \\ A^{(0)}_4 \\ A^{(N+1)}_1 \\ A^{(N+1)}_3 \end{pmatrix} = -\gamma\begin{pmatrix} A^d_1 \\ A^d_2 \\ A^d_3 \\ A^d_4 \end{pmatrix}, \tag{2.37}$$

which is solved by using standard matrix algebra.

Note, that the spontaneous emission is not coherent and thus the term $\gamma \mathbf{J}^d_{\downarrow}$ has to be added incoherently to the incident amplitude. Therefore we consider phases $e^{i\varphi_1}$, $e^{i\varphi_2}$, $e^{i\varphi_3}$, and $e^{i\varphi_4}$ of the source vector on the rigth side of Eq.(2.37)

$$\begin{pmatrix} A_1^d \\ A_2^d \\ A_3^d \\ A_4^d \end{pmatrix} \rightarrow \begin{pmatrix} e^{i\varphi_1} A_1^d \\ e^{i\varphi_2} A_2^d \\ e^{i\varphi_3} A_3^d \\ e^{i\varphi_4} A_4^d \end{pmatrix} = e^{i\varphi_1} \begin{pmatrix} A_1^d \\ e^{i(\varphi_2-\varphi_1)} A_2^d \\ e^{i(\varphi_3-\varphi_1)} A_3^d \\ e^{i(\varphi_4-\varphi_1)} A_4^d \end{pmatrix} \equiv e^{i\varphi_1} \begin{pmatrix} A_1^d \\ e^{i\Delta\varphi_2} A_2^d \\ e^{i\Delta\varphi_3} A_3^d \\ e^{i\Delta\varphi_4} A_4^d \end{pmatrix}. \tag{2.38}$$

Let us distinguish between two cases. By averaging outside Stokes vector components over all phases $\Delta\varphi_2$, $\Delta\varphi_3$, and $\Delta\varphi_4$

$$S^{\uparrow,\downarrow}_{out} = \left\langle S^{\uparrow,\downarrow}_{out}\left(\Delta\varphi_2,\, \Delta\varphi_3,\, \Delta\varphi_4\right)\right\rangle_{\Delta\varphi_2,\,\Delta\varphi_3,\,\Delta\varphi_4}, \tag{2.39}$$

we obtain case of *source without prefered polarization*, which could be used in light sources without spin polarized current. This approach corresponds with [12], but Benisty considered coherence between incident and spontaneously emited field.

However, in the case of spin-polarized light emission, *particular optical polarizations are prefered*. Thus, $\varphi_2 = \varphi_4$ and let us $\varphi_1 = \varphi_3 = 0$. By averaging outside Stokes vector components over φ_2

$$S^{\uparrow,\downarrow}_{out} = \left\langle S^{\uparrow,\downarrow}_{out}\left(\Delta\varphi_2\right)\right\rangle_{\Delta\varphi_2}, \tag{2.40}$$

we obtain outside Stokes vector of the structure with totally polarized source.

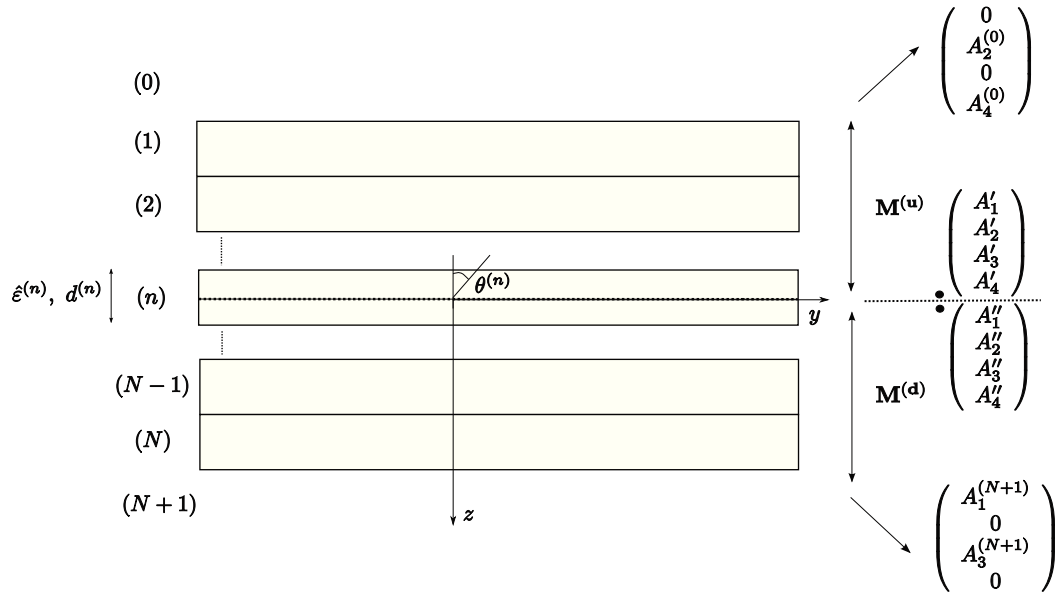

Figure 2.4: Anisotropic multilayer structure with isotropic active layer (n).

Chapter 3

Distribution of the source amplitude

Probability of the photon emission is related to the mechanism of the radiative recombination process and hence in most cases depends on the angle $\theta^{(n)}$. It is well established that emission in a semiconductor can be represented as an electric dipole emission in the weak coupoling regime. Electric dipole is a vectorial point source, which in bulk material can have any orientation. However, in quantum well structures, there is preference for emission through horizontal dipoles [16]. In this section, we will discuse the optical quantum selection rules for bulk and quantum well (QW) semiconductor structure. Because of the conservation of angular momentum, the circularly-polarized photons are emited. To model these transitions, we introduce system of two crossed linear sources (dipoles) with the phase shift $\pi/2$. This approach enables to find the source terms $\mathbf{J}_{\downarrow}^{d} = [A_1^d\, A_3^d]^T$ and $\mathbf{J}_{\uparrow}^{d} = [A_2^d\, A_4^d]^T$ of the active region, which amplify incident amplitudes as described by Eq.(2.34).

3.1 Quantum optical selection rules

The optical selection rules are given by evaluating the dipole moment of the transition between conduction band state $|c\rangle$ and valence band state $|v\rangle$ using the transition matrix element

$$\mathbf{D}_{cv} = \left\langle c|\hat{\mathbf{D}}|v\right\rangle, \tag{3.1}$$

where $\hat{\mathbf{D}}$ is the dipole moment operator. The Bloch states may be denoted using $|\mathbf{J},\, m_j\rangle$, where $\mathbf{J}$ denotes the total angular momentum and its projection onto the z axis is described by the magnetic quantum number m_j. The conduction band is represented by

two states $|1/2, \pm 1/2\rangle$, while the valence band is represented by two heavy hole states $|1/2, \pm 3/2\rangle$ and two light hole states $|1/2, \pm 1/2\rangle$. Let us have the quantization axis along the wavevector $\mathbf{k}$ and the crystal axis of the cubic $A^{III}B^{V}$ crystal (001) in the z direction. An electron state in the Γ-point of the conduction band can be described using the Bloch wave function

$$\psi^c_{km} = u_m e^{i\mathbf{k'r}}, \tag{3.2}$$

where the Bloch amplitudes have the folowing form

$$u^c_{1/2} = |S\uparrow\rangle, \quad u^c_{-1/2} = |S\downarrow\rangle. \tag{3.3}$$

The $|S\rangle$ denotes the s-type wavefunction and arrows denote spin functions. The Bloch amplitudes of the valence band can be described using the p-type wavefunctions $|X\rangle$, $|Y\rangle$ and $|Z\rangle$ with symmetry in x, y, and z, respectively

$$u^{hh}_{3/2} = -\frac{1}{\sqrt{2}}\left(|X\uparrow\rangle + i|Y\uparrow\rangle\right) \tag{3.4}$$

$$u^{hh}_{-3/2} = \frac{1}{\sqrt{2}}\left(|X\downarrow\rangle - i|Y\downarrow\rangle\right) \tag{3.5}$$

$$u^{lh}_{1/2} = \frac{1}{\sqrt{3}}\left[-\frac{1}{\sqrt{2}}\left(|X\downarrow\rangle + i|Y\downarrow\rangle\right) + \sqrt{2}|Z\uparrow\rangle\right] \tag{3.6}$$

$$u^{lh}_{-1/2} = \frac{1}{\sqrt{3}}\left[\frac{1}{\sqrt{2}}\left(|X\uparrow\rangle - i|Y\uparrow\rangle\right) + \sqrt{2}|Z\downarrow\rangle\right]. \tag{3.7}$$

Using previous relations, one can calculate the matrix element of dipole moment between conduction and valence band, which corresponds to a classical dipoles representation emitting circular and linear polarization [17](see Table 1).

cb		$\langle 1/2, +1/2\|$	$\langle 1/2, +1/2\|$
hh	$\|3/2, +3/2\rangle$	$-\sqrt{1/2}(\hat{x} + i\hat{y})$	0
	$\|3/2, -3/2\rangle$	0	$\sqrt{1/2}(\hat{x} - i\hat{y})$
lh	$\|1/2, +1/2\rangle$	$\sqrt{2/3}\hat{z}$	$-\sqrt{1/6}(\hat{x} + i\hat{y})$
	$\|1/2, -1/2\rangle$	$\sqrt{1/6}(\hat{x} - i\hat{y})$	$\sqrt{2/3}\hat{z}$

Table 3.1: Matrix elements of the dipole moment $\mathbf{D}_{cv}/D$ [17].

As required for conservation of the angular momentum, radiative recombinations lead to emission of right- (σ^+) and left-circularly polarized photons (σ^-), which have a projection of their angular momentum on the direction of the $\mathbf{k}$ vector equal to ± 1, respectively.

Moreover, from intensity of dipoles follows, that the hh transition are three times more probable than lh transition. Note, that the transition probability is proportional to $|D_{cv}|^2$. Let us define normalized transition probabilities

$$\xi_{hh} = 3/4 \quad \xi_{lh} = 1/4 \quad \xi_{hh} + \xi_{lh} = 1. \tag{3.8}$$

Note, that in direct bulk semiconductor, hh and lh bands are degenerate at the $\Gamma -$ point and those rules are valid for all direction of the emission. In the case of the QW structure, the degeneracy between the hh and lh valence bands is lifted due to quantum confinement and in many cases occuring epitaxial strain. Moreover, this selection rules are valid only in the vertical (Faraday) geometry, where the carrier spin orientation and the photon emission are oriented perpendicular to the QW plane [17, 18].

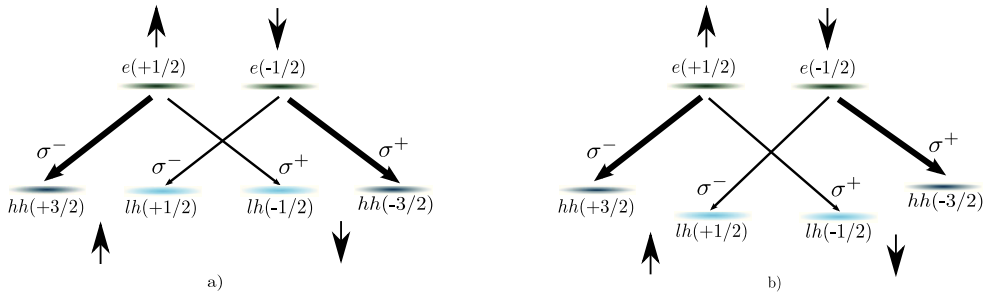

Figure 3.1: (a)Selection rules in direct bulk semiconductor. Transitions for which $\Delta m_j = +1$ and $\Delta m_j = -1$ result in the emission of circularly polarized photons with negative (σ^-) and positive (σ^+) helicity, respectively. Moreover, transitions involving heavy holes (hh) are three times more probable then those involving light holes (lh). When we consider 2D quantum system (b), the energetic splitting between hh and lh states appears as a consequence of the quantum confinement and epitaxial strain. In this case, the depicted selection rules are valid only for vertical geometry [17, 18].

3.2 Dipole radiation

Electric dipole is a vectorial point source, which in bulk material can have any orientation. However, in quantum well structures there is a preference for emission through horizontal

dipoles [16]. Note, that the vector of the electric field emitted by a dipole lies in the plane defined by vector **k** and vector of the dipole moment $\bar{\mu}$ [19]. The maximal field amplitude is emitted in the plane normal to the dipole moment $\bar{\mu}$ and drops sinusoidally to 0 for the direction of the dipole moment. Thus, in the case of the horizontal dipoles (plane xy parallel to the interfaces), we could decompose the total emitted field into two scalar cases: s-polarized and p-polarized fields generated by horizontal dipoles [12]

$$A_s^h = A\sin\varphi \tag{3.9}$$

$$A_p^h = A\cos\theta\cos\varphi = A\frac{k_z^{(n)}}{nk_0}\cos\varphi, \tag{3.10}$$

where φ and θ are the azimuth and the elevation, respectively. If we consider random randomly oriented dipoles, we could use an average of the amplitude over φ [20]

$$< P_s^h >= A^2 < \sin^2\varphi >= A^2\frac{1}{2\pi}\int\limits_0^{2\pi}\sin^2\varphi d\varphi = \frac{A^2}{2}$$

and

$$< P_p^h >= A^2\left[\frac{k_z^{(n)}}{nk_0}\right]^2 < \cos^2\varphi >= A^2\left[\frac{k_z^{(n)}}{nk_0}\right]^2\frac{1}{2\pi}\int\limits_0^{2\pi}\cos^2\varphi\mathrm{d}\varphi = \frac{\mathrm{A}^2}{2}\left[\frac{\mathrm{k_z^{(n)}}}{\mathrm{nk_0}}\right]^2.$$

Thus, we obtain

$$A_s^h = \frac{A}{\sqrt{2}} \tag{3.11}$$

$$A_p^h = \frac{A}{\sqrt{2}}\cos^{(n)}\varphi = \frac{A}{\sqrt{2}}\frac{k_z^{(n)}}{nk_0}. \tag{3.12}$$

We can express total radiated power through 4π sr

$$P_{s\,total}^h = \int\limits_\Omega \frac{A^2}{2}d\Omega' = \frac{A^2}{2}\int\limits_{4\pi} d\Omega' = 2\pi A^2$$

$$P_{p\,total}^h = \int\limits_\Omega \frac{A^2}{2}\cos^2\theta d\Omega' = \frac{2}{3}\pi A^2$$

To obtain normalized field amplitudes, let us consider total radiated power through $4\pi\,sr$ as 1

$$P_{total}^h = P_{s\,total}^h + P_{p\,total}^h = 2\pi A^2 + \frac{2}{3}\pi A^2 \equiv 1 \;\Rightarrow\; A = \pm\sqrt{\frac{3}{8\pi}}.$$

Thus, final normalized field amplitudes are [12]

$$A_s^h = \pm\sqrt{\frac{3}{16\pi}} \tag{3.13}$$

$$A_p^h = \pm\sqrt{\frac{3}{16\pi}}\cos\theta = \pm\sqrt{\frac{3}{16\pi}}\,\frac{k_z^{(n)}}{nk_0}\,. \tag{3.14}$$

This approach enables calculation of the outside field amplitude of the classical RCLED anisotropic structures, where active layer emitts linearly polarized photons.

3.3 Method of two-crossed linear sources

First let us consider that emission probability of the circularly polarized photon is angular independent. Hence, for right- and left-circularly polarized waves propagating in the $+z$ ($\downarrow$) and $-z$ ($\uparrow$) direction, respectively, we obtain source Jones vectors in the form

$$\mathbf{J}^d_{\downarrow,R} = \mathbf{J}^d_{\uparrow,R} = \begin{pmatrix} 1 \\ i \end{pmatrix} \tag{3.15}$$

$$\mathbf{J}^d_{\downarrow,L} = \mathbf{J}^d_{\uparrow,L} = \begin{pmatrix} 1 \\ -i \end{pmatrix}. \tag{3.16}$$

In other words, as described in previous section, circularly polarized part of incident waves, which travel through the active plane, are amplified (see Eq.(2.34)). Imaginary unit i represents $\pi/2$ phase shifting between two orthogonal (s- and p-polarized) linear waves.

3.4 General appproach

Both photon emission probability and photon polarization in most cases depend on the angle $\theta^{(n)}$ and are related to the mechanism of the radiative recombination and to the parameters of the structures. Thus, it could be very useful to introduce general parametrized function of the amplitude dependence on the emission angle $\theta^{(n)}$. In the case of QW structure, where most energy is emitted in the direction normal to the plane, we introduce

paremetrization of the source Jones vectors $\mathbf{J}^d_{\downarrow,R}$ (3.15) and $\mathbf{J}^d_{\downarrow,R}$ (3.16)

$$\mathbf{J}^d_{\downarrow,R} = \begin{pmatrix} \mathcal{A}^{\downarrow}_s + \mathcal{B}^{\downarrow}_s \cos^l\theta^{(n)} \\ i\left(\mathcal{A}^{\downarrow}_p + \mathcal{B}^{\downarrow}_p \cos^l\theta^{(n)}\right) \end{pmatrix} \quad \mathbf{J}^d_{\uparrow,L} = \begin{pmatrix} \mathcal{A}^{\uparrow}_s + \mathcal{B}^{\uparrow}_s \cos^l\theta^{(n)} \\ -i\left(\mathcal{A}^{\uparrow}_p + \mathcal{B}^{\uparrow}_p \cos^l\theta^{(n)}\right) \end{pmatrix} \tag{3.17}$$

and

$$\mathbf{J}^d_{\uparrow,R} = \begin{pmatrix} \mathcal{A}^{\uparrow}_s + \mathcal{B}^{\uparrow}_s \cos^l\theta^{(n)} \\ i\left(\mathcal{A}^{\uparrow}_p + \mathcal{B}^{\uparrow}_p \cos^l\theta^{(n)}\right) \end{pmatrix} \quad \mathbf{J}^d_{\downarrow,L} = \begin{pmatrix} \mathcal{A}^{\downarrow}_s + \mathcal{B}^{\downarrow}_s \cos^l\theta^{(n)} \\ -i\left(\mathcal{A}^{\downarrow}_p + \mathcal{B}^{\downarrow}_p \cos^l\theta^{(n)}\right) \end{pmatrix}, \tag{3.18}$$

where $\mathcal{A}$, $\mathcal{B}$ and l are the nonnegative parameters, which could be determined using theory or obtained from fit of experimental data. Note, that from symmetry reason is sufficient to let $\theta^{(n)} \in < 0, \pi/2 >$.

Let us combine this approach together with the quantum selection rules depicted in Fig. 3.1. The source vectors $\mathbf{J}^d_{\uparrow,R}$ and $\mathbf{J}^s_{\downarrow,L}$ (3.18) correspond with a transitions $\Delta m_j = +1$ resulting in the emission of circularly polarized photons with negative helicity (σ^-) when propagating in the $+z$ direction ($\downarrow$) but positive helicity (σ^+) for $-z$ direction ($\uparrow$). If we consider symmetry of the source

$$\mathcal{A}^{\downarrow}_s + \mathcal{B}^{\downarrow}_s \cos^l\theta^{(n)} = \mathcal{A}^{\uparrow}_s + \mathcal{B}^{\uparrow}_s \cos^l\theta^{(n)} = \mathcal{A}_s + \mathcal{B}_s \cos^l\theta^{(n)} \tag{3.19}$$

and

$$\mathcal{A}^{\downarrow}_p + \mathcal{B}^{\downarrow}_p \cos^l\theta^{(n)} = \mathcal{A}^{\uparrow}_p + \mathcal{B}^{\uparrow}_p \cos^l\theta^{(n)} = \mathcal{A}_p + \mathcal{B}_p \cos^l\theta^{(n)}, \tag{3.20}$$

the number of parameters is reduced and source vector has folowing form

$$\mathbf{J}^d_{\uparrow} = \mathbf{J}^s_R = \begin{pmatrix} \mathcal{A}_s + \mathcal{B}_s \cos^l\theta^{(n)} \\ i\left(\mathcal{A}_p + \mathcal{B}_p \cos^l\theta^{(n)}\right) \end{pmatrix} \quad \mathbf{J}^d_{\downarrow} = \mathbf{J}^s_L = \begin{pmatrix} \mathcal{A}_s + \mathcal{B}_s \cos^l\theta^{(n)} \\ -i\left(\mathcal{A}_p + \mathcal{B}_p \cos^l\theta^{(n)}\right) \end{pmatrix}. \tag{3.21}$$

Similarly, for $\Delta m_j = -1$ transitions we obtain

$$\mathbf{J}^d_{\downarrow} = \mathbf{J}^s_R = \begin{pmatrix} \mathcal{A}_s + \mathcal{B}_s \cos^l\theta^{(n)} \\ i\left(\mathcal{A}_p + \mathcal{B}_p \cos^l\theta^{(n)}\right) \end{pmatrix} \quad \mathbf{J}^d_{\uparrow} = \mathbf{J}^s_L = \begin{pmatrix} \mathcal{A}_s + \mathcal{B}_s \cos^l\theta^{(n)} \\ -i\left(\mathcal{A}_p + \mathcal{B}_p \cos^l\theta^{(n)}\right) \end{pmatrix}. \tag{3.22}$$

In the special case, when circularly polarized waves is considered in all direction, the elements of the source vectors have simple form

$$\mathcal{A}_s + \mathcal{B}_s \cos^l\theta^{(n)} = \mathcal{A}_p + \mathcal{B}_p \cos^l\theta^{(n)} = \mathcal{A} + \mathcal{B} \cos^l\theta^{(n)}. \tag{3.23}$$

Note that if we use parameters $l = 1$, $A_p = B_s = 0$ in (3.18) and (3.17), we obtain situation of two crossed electric dipoles with a relative phase difference $\pi/2$. This source emits circularly polarized wave in the direction orthogonal to the plane of these dipoles (z

axis). Polarization changes from circularly through elliptical to linear in the direction of the dipoles.

Recal from previous section that transition involving heavy holes are three times more probable then those involving light holes. For example, if we inject carriers with 100% spin polarization in $m_j = 1/2$ state, the emited photons consists both of photons with positive (σ^-) and negative (σ^-) helicity, while the intensity of σ^- is three times stronger(in the $+z$ direction $\downarrow$). Denoting $n_\pm$ the densities of electrons in the $\pm 1/2$ electron states, we can use following combination of the dipole sources.

$$\begin{aligned}
A^d_{\downarrow\uparrow} &= \frac{n_+}{n_+ + n_-}\left[\sqrt{\xi_{hh}}\begin{pmatrix} 1 \\ i\cos\theta^{(n)} \end{pmatrix} + e^{i\varphi}\sqrt{\xi_{lh}}\begin{pmatrix} 1 \\ -i\cos\theta^{(n)} \end{pmatrix}\right] + \\
&+ \frac{n_-}{n_+ + n_-}\left[\sqrt{\xi_{lh}}\begin{pmatrix} 1 \\ i\cos\theta^{(n)} \end{pmatrix} + e^{i\varphi}\sqrt{\xi_{hh}}\begin{pmatrix} 1 \\ -i\cos\theta^{(n)} \end{pmatrix}\right] = \qquad (3.24) \\
&= \frac{1}{n_+ + n_-}\begin{pmatrix} n_+\sqrt{\xi_{hh}} + n_-\sqrt{\xi_{lh}} + e^{i\varphi}\left(n_+\sqrt{\xi_{lh}} + n_-\sqrt{\xi_{hh}}\right) \\ i\cos\theta^{(n)}\left(n_+\sqrt{\xi_{hh}} + n_-\sqrt{\xi_{lh}} - e^{i\varphi}\left(n_+\sqrt{\xi_{lh}} + n_-\sqrt{\xi_{hh}}\right)\right) \end{pmatrix} \qquad (3.25) \\
&\equiv \frac{hh}{n_+ + n_-}\begin{pmatrix} n_R + e^{i\varphi}n_L \\ i\cos\theta^{(n)}\left(n_R - e^{i\varphi}n_L\right) \end{pmatrix}, \qquad (3.26)
\end{aligned}$$

where ξ_{lh} and ξ_{hh} are normalized transition probabilities defined by Eq.(3.8). Let us define the effective polarization degree of emited photons

$$P' = \frac{n_R - n_L}{n_R - n_L} = \frac{\sqrt{\xi_{hh}} - \sqrt{\xi_{lh}}}{\sqrt{\xi_{hh}} + \sqrt{\xi_{lh}}}\,\frac{n_+ - n_-}{n_+ + n_-}\,, \qquad (3.27)$$

which is in the form of the product of the degree of transition probabilities and the spin polarization of carriers

$$P = \frac{n_+ - n_-}{n_+ + n_-}\,. \qquad (3.28)$$

We let $\theta^{(n)} \in < 0, \pi/2 >$ and $\theta^{(n)} \in < \pi, \pi/2 >$ for $A_\uparrow$ and $A_\downarrow$, respectively. By averaging final Stokes intensities over φ, we describe independence of hh and lh transitions. Note, that the quantization axis is along the $+z$ direction ($\downarrow$).

Chapter 4

Models

In this chapter we demonstrate the theory on practical structures of multilayers with diferent dipole sources. First we demonstrate basic aspects on simplified symmetric structure with different Jones source vectors. In the next step, more realistic half spin-VCSEL structure is modeled.

4.1 Simple multilayer structure with source layer

Figure 4.1 shows schematically modeled structure including source dipole layer in the center. Thicknesses of the films are $d^{(1)} = d^{(3)} = \lambda/n^{(1)} = \lambda/n^{(3)}$ and $d^{(2)} = 2\lambda/n^{(2)}$, where $\lambda = 860$ nm. Light emitted from the structure as a function of the angle from surface normal $\theta^{(0)}$ is calculated using Eqs. (2.37) (3.3) in terms of Stokes vectors.

Figures 4.2a and b show special case of isotropic system with the source layer emitting pure s- and p- polarizations $\mathbf{J}^s_\uparrow = \mathbf{J}^s_\downarrow = [1\ 0]^T$ and $\mathbf{J}^s_\uparrow = \mathbf{J}^s_\downarrow = [0\ 1]^T$, respectively.

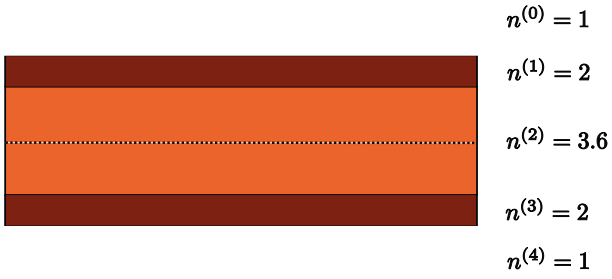

Figure 4.1: Modeled structure shown schematically

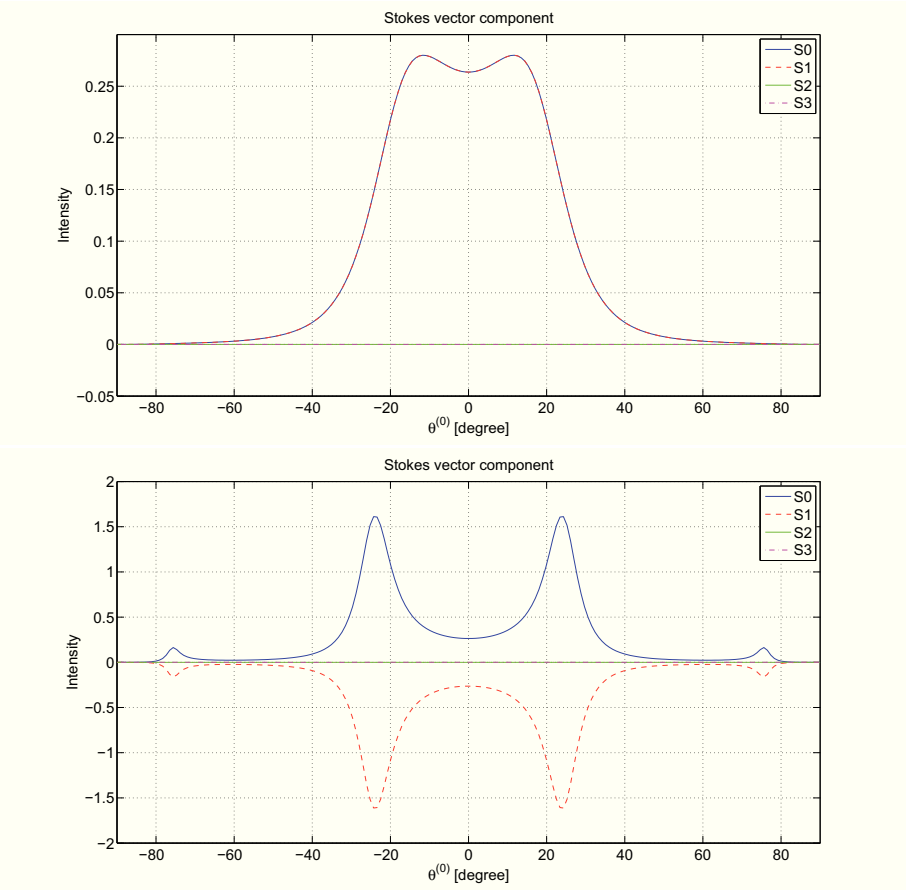

Figure 4.2: Special isotropic case with the source layer emitting pure s- and p- polarizations.

Figure 4.3a shows special case of isotropic system with the source layer emitting pure circular polarizations described using the Jones vectors $\mathbf{J}^s_{\uparrow} = [1 \; i]^T$ and $\mathbf{J}^s_{\downarrow} = [1 \; -i]^T$. Figure 4.3b shows radiation of the structure with the source emiting circular polarization of oposite handness described using the Jones vectors $\mathbf{J}^s_{\uparrow} = [1 \; -i]^T$ and $\mathbf{J}^s_{\downarrow} = [1 \; i]^T$. Emitted light from the structure is partially polarized as shown in Figure 4.3c.

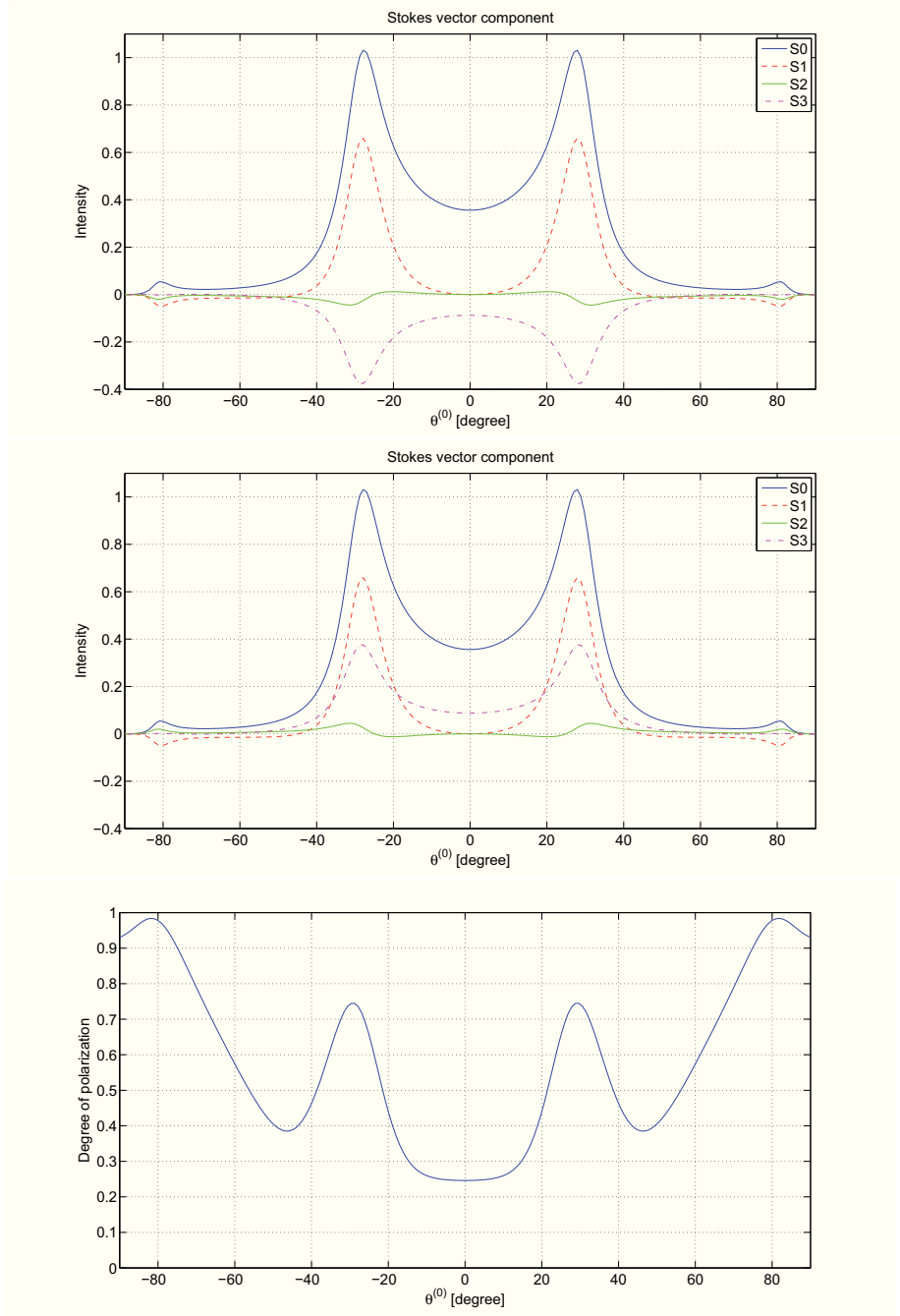

Figure 4.3: Structure with the source layer emitting right and left handed circular polarizations. Polarization degree of emited light is shown as a function of emitting angle.

4.2 Realistic half spin-VCSEL

For the following model, Jones source vector (3.26) will be used. Figure 4.4 shows schematically modeled structure including electrode (Au), magneto-optical spin-injection layer (Co) in polar geometry $\varepsilon_{12}^{(Co)} = -\varepsilon_{21}^{(Co)} = -0.2i$, tunnel barrier (MgO), active layer GaAs with active plane in the center and Bragg structure. This structure is part of so-called half spin-VCSEL, where the external mirror could be used. The wavelength of the emitted light is $\lambda = 860$ nm. Optical constants are $n^{(\mathrm{Au})} = 0.23 + i5.68$, $n^{(\mathrm{Co})} = 3.82 + i4.84$, $n^{(\mathrm{MgO})} = 1.73$, and $n^{(\mathrm{GaAs})} = 3.66$ [21, 22].

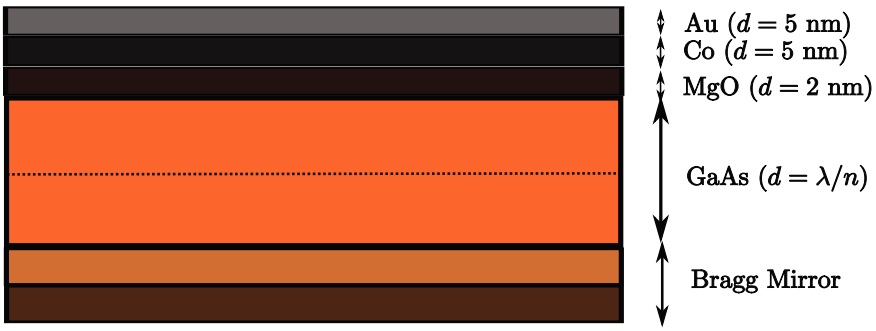

Figure 4.4: Modeled spin-structure shown schematically including the gold electrode (Au), magneto-optical spin-injection layer (Co), tunnel barrier (MgO), active layer GaAs with active plane in the center and Bragg structure.

Figures 4.5 and 4.6 demonstrate changes of the Stokes vector components during varying of the injected spin polarization defined by Eq (3.28). One can see, that total intensity S_0 and component S_1 do not change, but components S_2 and S_3 switch signs due to different transition probabilities. Experimental measurment of the Stokes vector can thus bring valuable information about injected spin polarized current. Maximal field is emitted in the case of $\theta^{(0)} = 18°$. This could be explained as an interference effect. Degree of polarization shows depolarization effect which is caused by incoherent summation of spontaneously emitted waves propagating in the direction up and down. As can be seen on Figure 4.8, thickness of the GaAs film has crucial impact on extracted light due to the interference effects. Figures 4.9 and 4.10 show effects of the weight coefficients of spontaneous emission γ and stimulated emission δ, respectively. While γ does not significantly change the emited pattern but has impact on the total intensity, δ enhances significantly resonant peaks and thus changes the emitted pattern.

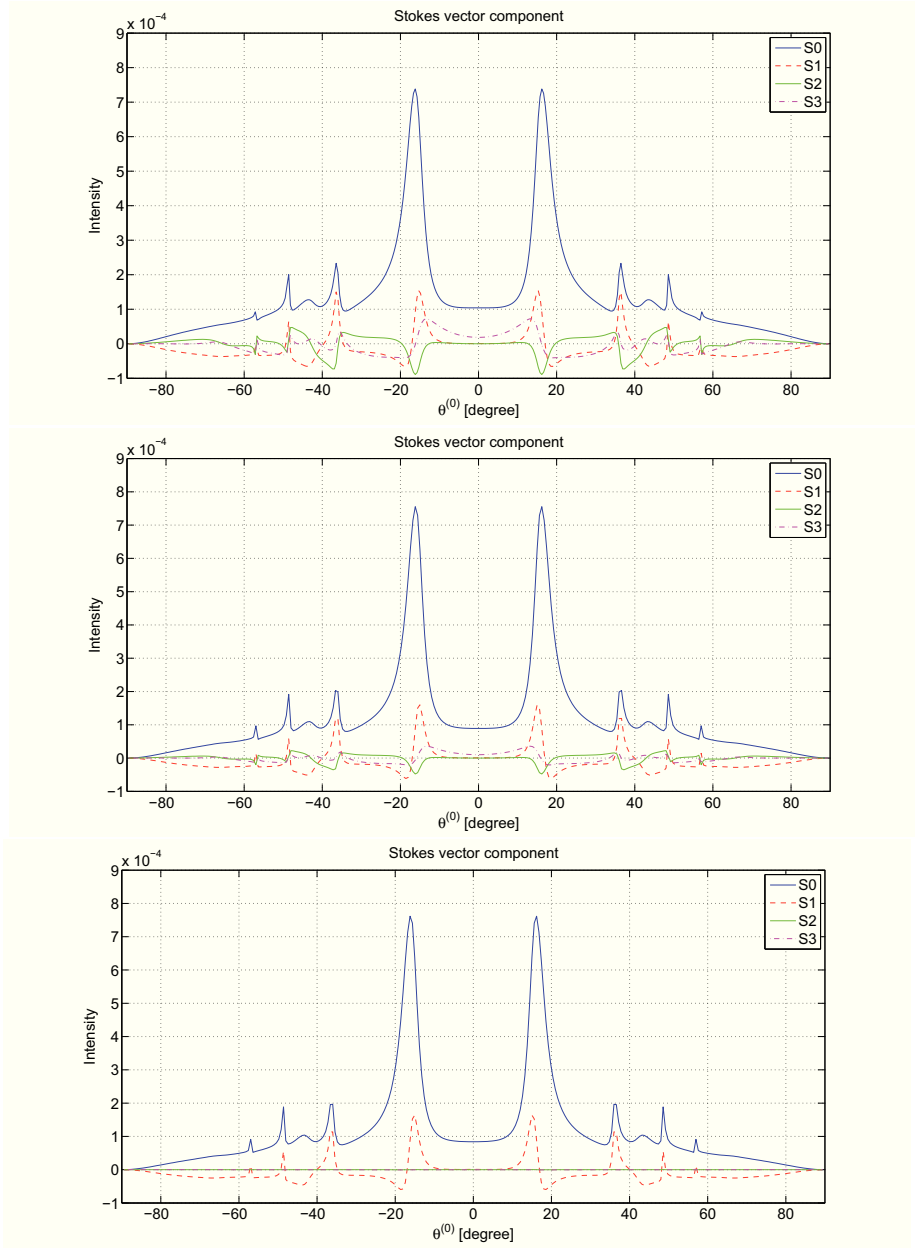

Figure 4.5: The effect of the electron spin polarization. Subplots show emission pattern for varying injected spin polarization $P = 1$, $P = 0.5$, and $P = 0$.

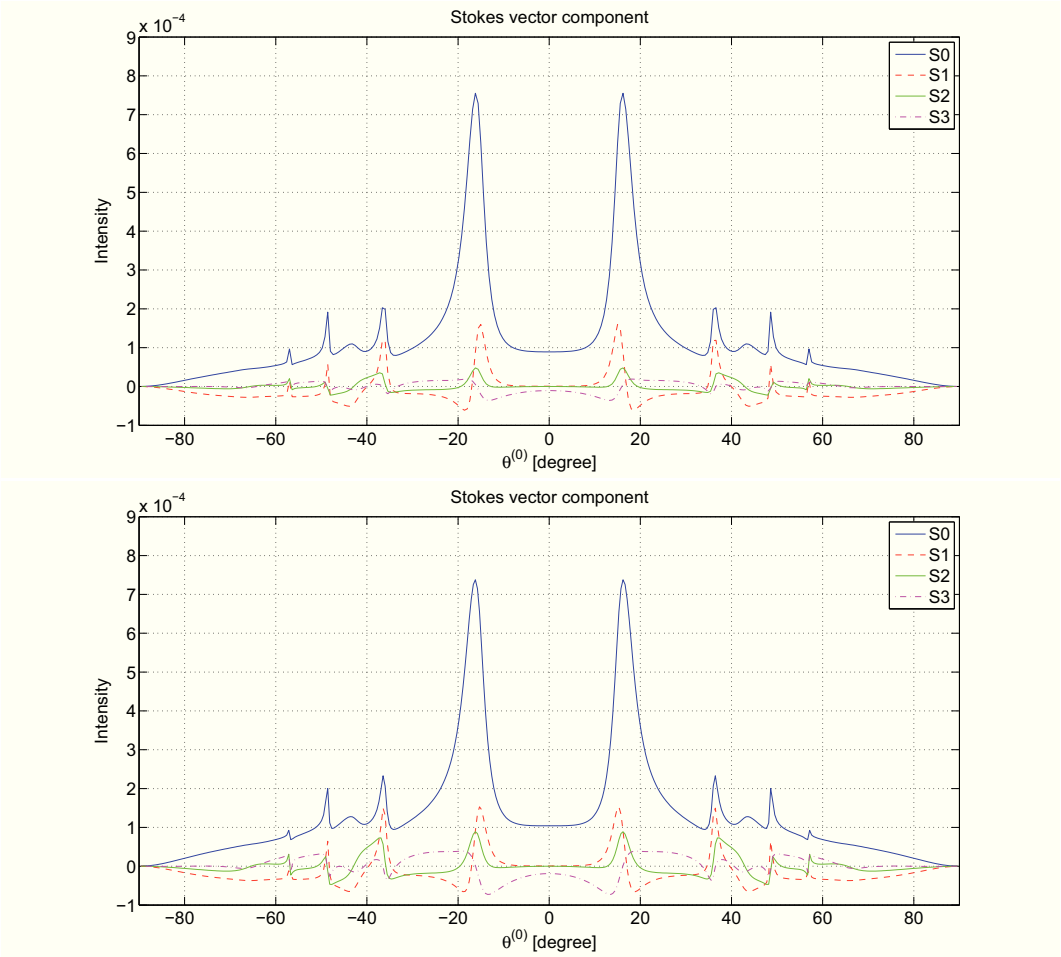

Figure 4.6: Continuation of Fig. 4.5. Subplots show emission pattern for varying injected spin polarization $P = -0.5$ and $P = -1$.

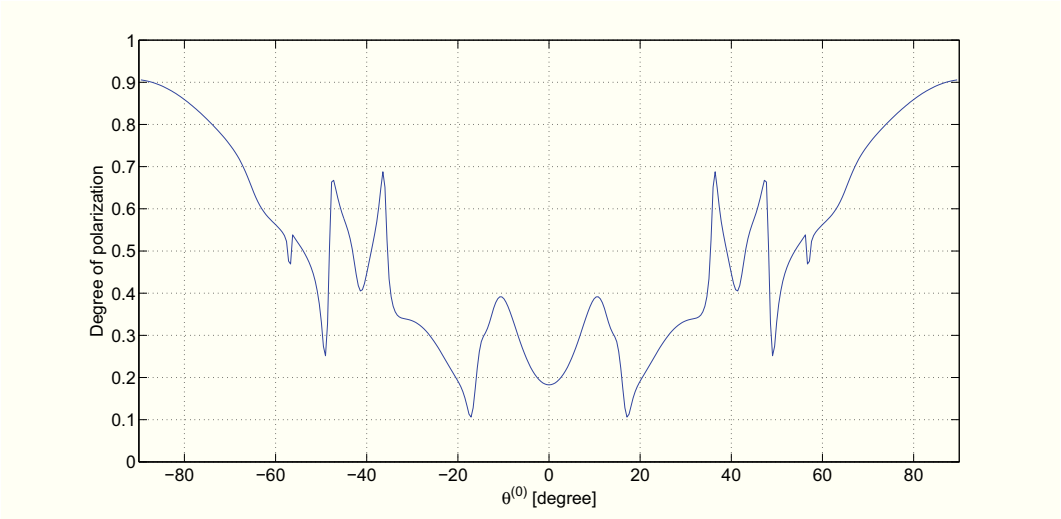

Figure 4.7: Degree of polarization of the emitted light in the case $P = 1$.

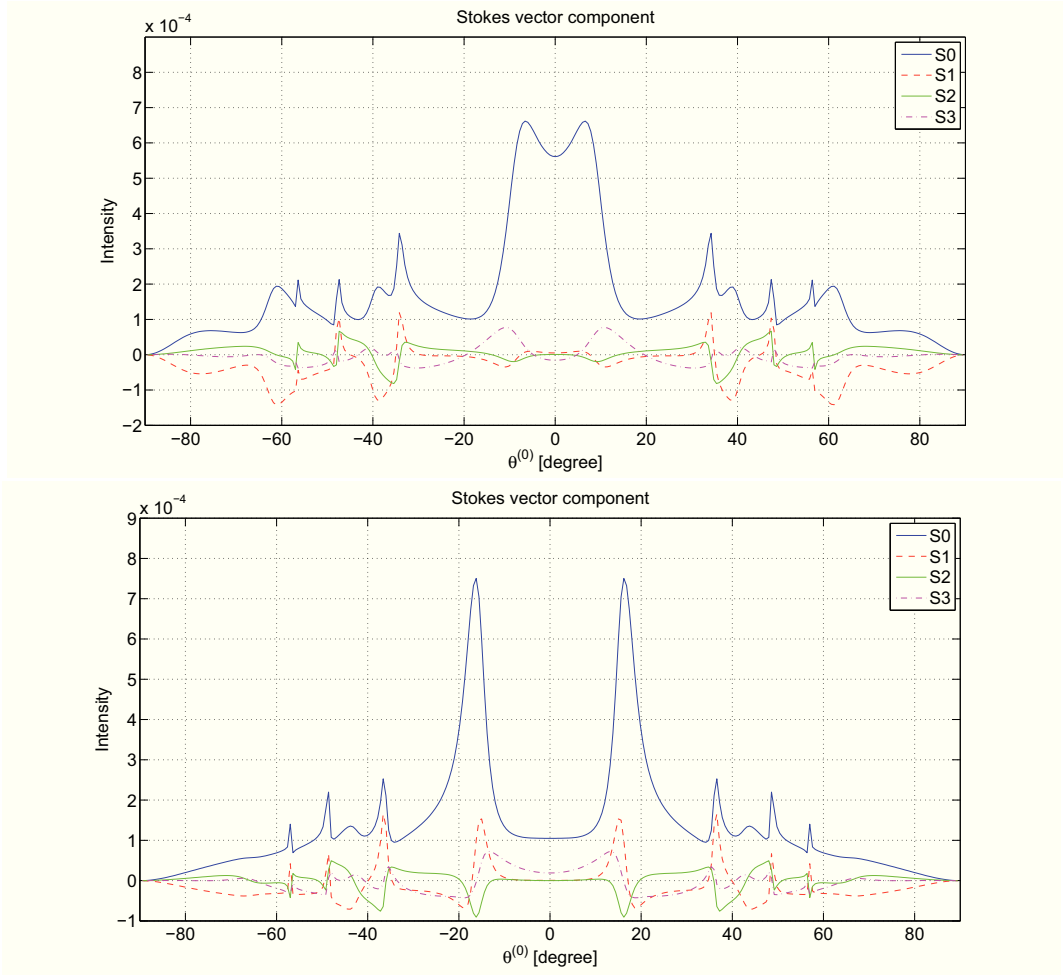

Figure 4.8: Effect of thickness $d^{(n)}$. Subplot a $d^{(n)} = \lambda/3n^{(n)}$ and subplot b $d^{(n)} = \lambda/4n^{(n)}$.

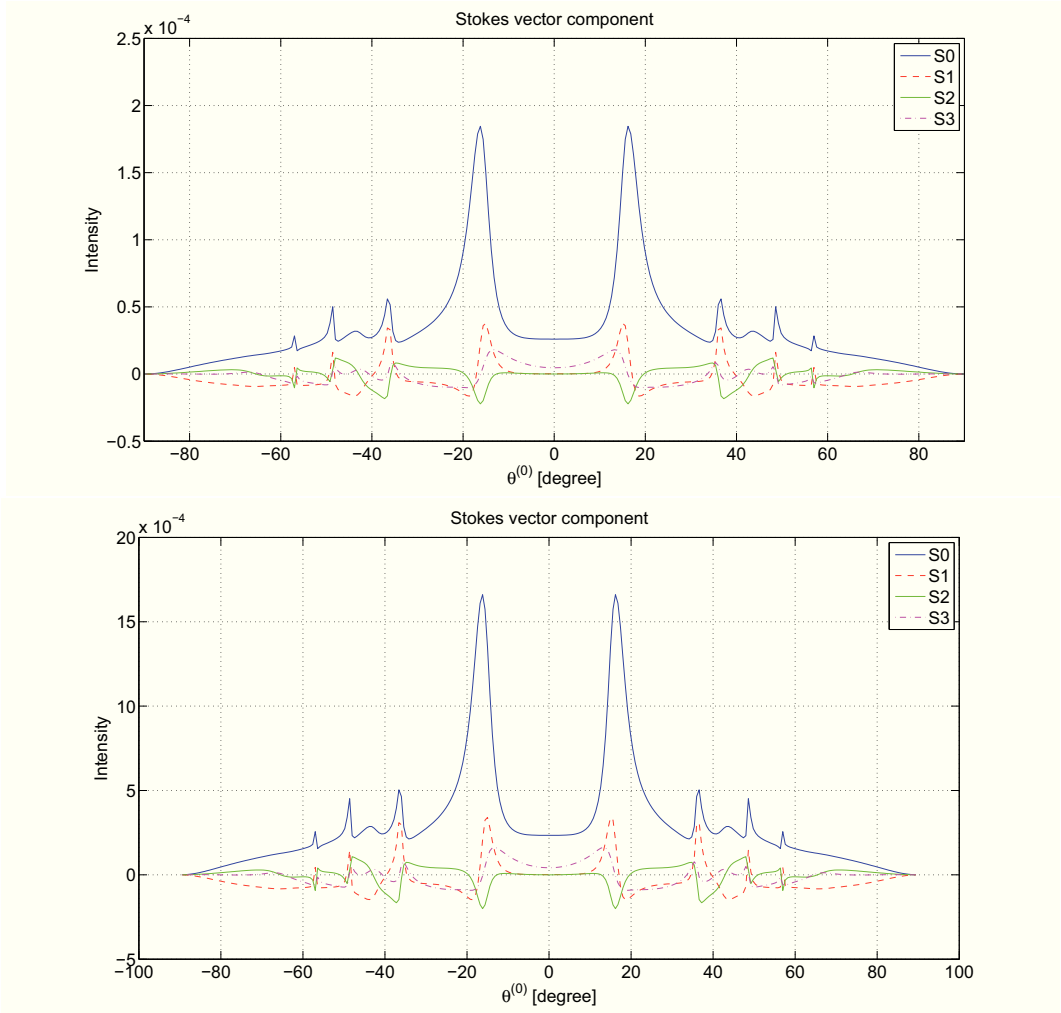

Figure 4.9: Effect of the weight coefficient of spontaneous emission γ. Subplot a $\gamma = 0.2$ and subplot b $\gamma = 0.6$.

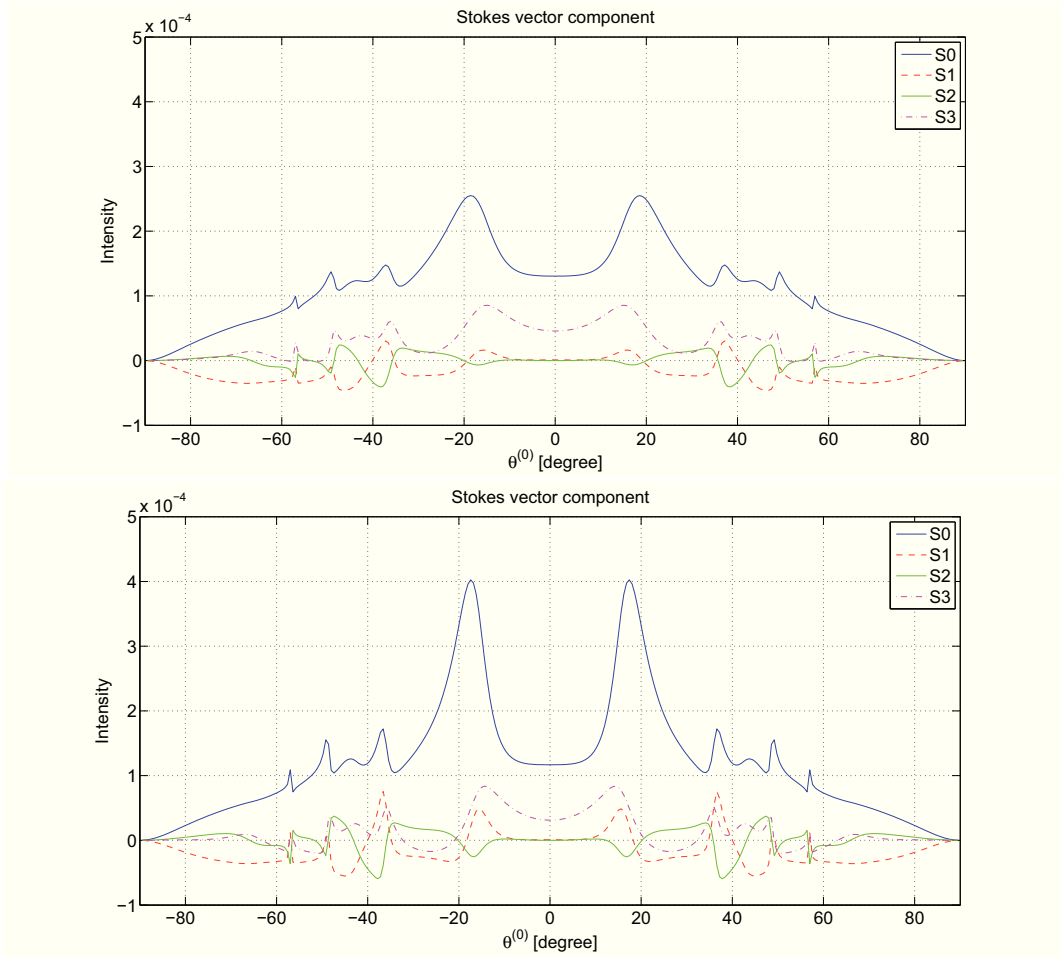

Figure 4.10: Effect of the weight coefficient of stimulated emission δ. Subplot a $\delta = 0.2$ and subplot b $\delta = 0.6$.

Chapter 5

Conclusion

This thesis enabled me to study interesting part of modern physics including spin-polarized light sources.

The main contribution of this diploma thesis is development of the new approach for modeling spin-polarized LEDs and spin-VCSELs:

- modeling of light emission in resonant multilayer structure by using generalized 4×4 matrix approach fulfilling Maxwell equations in each layer and boundary conditions for electromagnetic field
- representation of active layer by using two crossed dipole sources, which are directly related to the quantum optical selection rules
- numerical demonstration of the approach on the half spin-VCSEL structure

Theoretical results is going to be published in a journal with impact factor. Main goals for future work

- application of the formalism to the more complex structure such as spin-VCSEL with multiple quantum wells
- experimental study of spin-VCSELs structures and fitting experimental data to model
- study and modeling of quantum transition in more complex structures with spin-polarized electric and polarized optical pumping

To continue my research in this part of physics, I would like to apply for joint PhD study at VŠB-TUO, Ostrava and at Unité Mixte de Physique CNRS/Thales, Paris.

Bibliography

[1] FIEDERLING R.; KEIM, M.; REUSCHER, G.; OSSAU, G.; SCHMIDT, G.; WAAG, A. and MOLENKAMP, L.W. Injection and detection of a spin-polarized current in a light-emitting diode. *Nature*, vol. 402, no. 6763, pp. 787–790, 1999.

[2] ZHU, H.J.; RAMSTEINER M.; KOSTIAL, H.; WASSERMEIER, M.; SCHÖNHERR, H.P. and PLOOG, K. H. Room-temperature spin injection from Fe into GaAs. *Phys. Rev. Lett.*, vol. 87, p. 016601, Jun 2001.

[3] ADELMANN, C.; LOU, X.; STRAND, J.; C. J. Palmstrøm; and P. A. Crowell. Spin injection and relaxation in ferromagnet-semiconductor heterostructures. *Phys. Rev. B*, vol. 71, p. 121301, Mar 2005.

[4] HOVEL, S.; GERHARDT, N. C.; HOFMANN, M. R.; LO, F.-Y.; LUDWIG, A.; REUTER, D.; WIECK, A. D.; SCHUSTER, E.;WENDE, H.; KEUNE, W.; PETRACIC, O. and WESTERHOLT, K. Room temperature electrical spin injection in remanence. *Applied Physics Letters*, vol. 93, no. 2, p. 021117, 2008.

[5] RUDOLPH, J.; DOHRMAN, S.; HAGELE, D.; OESTREICH, M.; STOLZ W. Room-temperature threshold reduction in vertical-cavity surface-emitting lasers by injection of spin-polarized electrons. *Applied Physics Letters*, vol. 87, no. 24, p. 241117, 2005.

[6] HOLUB, M. and JONKER B. T. Threshold current reduction in spin-polarized lasers: Role of strain and valence-band mixing. *Phys. Rev. B*, vol. 83, p. 125309, Mar 2011.

[7] LEE, J.;FALLS, W.; OSZWALDOWSKI, R. and ZUTIC, I. Spin modulation in semiconductor lasers. *Applied Physics Letters*, vol. 97, no. 4, p. 041116, 2010.

[8] ANDO, H.; SOGAWA, T. and GOTOH, H. Photon-spin controlled lasing oscillation in surface-emitting lasers. *Applied Physics Letters*, vol. 73, no. 5, pp. 566–568, 1998.

[9] HOVEL, S.; BISCHOFF, A.; GERHARDT, N. C.; HOFMANN, M. R.; ACKEMANN, T.; KRONER, A. and MICHALZIK R. Optical spin manipulation of electrically pumped vertical-cavity surface-emitting lasers. *Applied Physics Letters*, vol. 92, no. 4, p. 041118, 2008.

[10] SIEGMAN, A. E. *Lasers*. University Science Books, 1986.

[11] YOKOYAMA, H.; NISHI, K.; ANAN, T.; YAMADA, H.; BRORSON, S. D. and IPPEN, E. P. Enhanced spontaneous emission from gaas quantum wells in monolithic microcavities. *Applied Physics Letters*, vol. 57, no. 26, pp. 2814–2816, 1990.

[12] BENISTY, H.; STANLEY, R. and MAYER, M. Method of source terms for dipole emission modification in modes of arbitrary planar structures. *J. Opt. Soc. Am. A*, vol. 15, pp. 1192–1201, May 1998.

[13] YEH, P. Electromagnetic propagation in birefringent layered media. *J. Opt. Soc. Am.*, vol. 69, pp. 742–755, 1979.

[14] AZZAM, R. M. A. and BASHARA, N. M. *Ellipsometry and Polarized Light*. Amsterdam: North-Holland, 2nd ed., 1987.

[15] VIŠŇOVSKÝ, Š. Magneto-optical ellipsometry. *Czech. J. Phys. B*, vol. 36, pp. 625–650, 1986.

[16] YAMANISHI, M. and SUEMUNE, I. Comment on polarization dependent momentum matrix elements in quantum well lasers. *Japanese Journal of Applied Physics*, vol. 23, no. Part 2, No. 1, pp. L35–L36, 1984.

[17] MEIER, F. and ZAKHARCHENYA, B. *Optical orientation*. Modern problems in condensed matter sciences, North-Holland, 1984.

[18] HOLUB, M. and BHATTACHARYA, P. Spin-polarized light-emitting diodes and lasers. *Journal of Physics D: Applied Physics*, vol. 40, no. 11, p. R179, 2007.

[19] BLADEL, J. *Electromagnetic Fields*. IEEE Press Series on Electromagnetic Wave Theory, Wiley-Interscience, 2007.

[20] BAETS, R.; BIENSTMAN, P. and BOCKSTAELE, R. Basics of dipole emission from a planar cavity. *Confined Photon Systems* (H. Benisty, C. Weisbuch, c. Polytechnique, J.-M. Gérard, R. Houdré, and J. Rarity, eds.), vol. 531 of *Lecture Notes in Physics*, pp. 38–79, Springer Berlin / Heidelberg, 1999. 10.1007/BFb0104380.

[21] PALIK, E. D. ed., *Handbook of Optical Constants of Solids I, II, III.* Academic Press, 1991.

[22] BASS, M.; DECUSATIS, C.; ENOCH, J.; LAKSHMINARAYANAN, V.; LI, G.; MACDONALD, C.; MAHAJAN, V. and STRYLAND, E. *Handbook of Optics, Third Edition Volume IV: Optical Properties of Materials, Nonlinear Optics, Quantum Optics (set).* Handbook of Optics, McGraw-Hill Education, 2009.

Acknowledgments

I am heartily thankful to my supervisor, doc.Dr.Mgr.Kamil Postava from Department of Physics at the Technical University of Ostrava, whose support and guidance enabled me to develop an understanding of the interesting part of physics. I would like to thank to Dr. Henri Jaffrès from Unité Mixte de Physique CNRS/Thales, Paris for motivation to research amazing subject of spin-polarized light-emitting structures.